

Large-Diameter 3C-SiC/Si Hetero-Epitaxial Substrates and Thick, High-Quality GaN Epitaxial Layers Grown on These Substrates for GaN Power Applications

Keisuke Kawamura¹, Shigeomi Hishiki¹, Hiroki Uratani¹, Sumito Ouchi¹, Hiroki Suzuki¹, Yoshiki Sakaida¹, Koichi Kitahara¹, Hirokazu Goto¹, and Ichiro Hide¹,
Shuichi Kaneko², Osamu Machida², and Toru Yoshie²

¹Air Water Inc.

2290-1, Toyoshinatakibe, Azumino, Nagano 399-8204, Japan
Phone: +81- 263-71-2510 E-mail: kawamura-kei@awi.co.jp

²Sanken Electric Co., LTD

3-6-3, Kitano, Niiza, Saitama 352-8666, Japan
Phone: +81-48-472-1111

Abstract

We have grown 8- μ m-thick nitride composite layers with a simple nitride buffer structure on 6" 3C-SiC/Si substrates. The 3C-SiC intermediate layer exhibited excellent effects for suppressing cracks and melt-back defects, even in the case of an 8- μ m-thick nitride structure and a practical 6" wafer. High-electron-mobility transistors (HEMTs) were fabricated on the wafers and practical off-leakage characteristics and current collapses were successfully confirmed.

1. Introduction

In the field of GaN-based high-power, high-frequency applications, GaN devices grown on Si substrates have been eagerly studied owing to their preferable features for commercialization, which include the ease of procurement of large-diameter starting wafers at low costs. However, direct epitaxy of GaN on Si substrates often results in a low crystalline quality and generation of cracks due to the large lattice mismatch between Si and GaN. Moreover, the occurrence of melt-back reactions due to the chemical instability of Si are also a considerable technical problem.

3C-SiC hetero-epitaxial growth technology on Si is a promising approach for addressing the above-mentioned technical hurdles [1]. 3C-SiC is the easiest poly-type to grow on Si, and the lattice mismatch of GaN/3C-SiC is approximately 3.5%, which is significantly smaller than that of GaN/Si. Furthermore, 3C-SiC is a refractory material that maintains chemical and mechanical stability in a high-temperature environment. Therefore, 3C-SiC leads to an improvement in the crystalline quality, inhibits the melt-back reaction, and reduces cracks [2] when it is used as an intermediate layer to grow GaN. A 3C-SiC intermediate layer as a nitride buffer considerably improved the current collapse characteristics [3]. The Air Water Group has paid attention to the above advantages and to the production of 3C-SiC (111)/Si substrates with diameters up to 8" using original epitaxial reactors in 2013 [4].

In this study, we have grown thick nitride composite layers on 3C-SiC/Si to achieve a high vertical breakdown voltage. As for the nitride thickness and wafer diameter, the applicable values for commercial AlGaIn/GaN HEMTs for

power applications were selected. We subsequently investigated their advantages on the same structure of nitride layers that were grown directly on Si substrates.

2. Nitride deposition and CANDELA CS20 analysis

We prepared commercial 6" Czochralski (Cz)-Si substrates and 1- μ m-thick 3C-SiC (111)/Si substrates [8]. To focus on the structural differences, the Cz-Si substrates and the starting wafers for SiC/Si have the same specifications. The 7- or 8- μ m-thick nitride composite layers shown in Fig.1 were then grown on those substrates via metal-organic chemical vapor deposition (MOCVD). By optimizing the nitride buffer structures and by using the Cz-Si crystal with a high elastic limit, the SORI after nitride deposition of both the 6" SiC/Si and the Si substrates was stably controlled to less than 50 μ m.

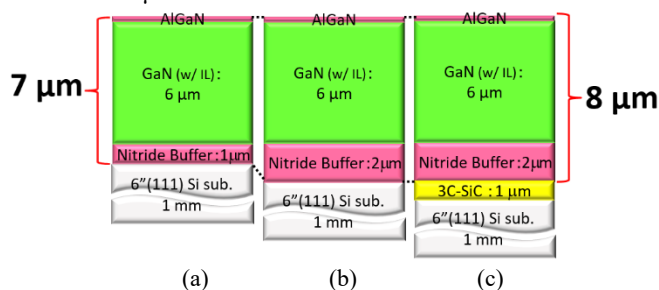


Fig.1 Schematic cross-sections of (a) 7- μ m-thick nitride on Si, (b) 8- μ m-thick nitride on Si, and (c) 8- μ m-thick nitride on SiC/Si.

After nitride deposition, the wafers were subjected to KLA-Tencor Candela CS20 analysis to detect cracks and melt-back defects. Figure 2 shows laser scattering images by CS20 for crack detection of the substrates (a)–(c) in Fig.1. In the 7- μ m-thick nitride on Si (substrate (a)), cracks with a length larger than 10 mm get generated from the outermost periphery of the wafer. In the 8- μ m-thick nitride on Si (substrate (b)), the cracks extended all over the wafer. In contrast, the 8- μ m-thick nitride on SiC/Si (substrate (c)) successfully attains to realize a crack-free surface with an edge exclusion of approximately 5 mm. Figure 3 shows extended laser scattering images by CS20 for melt-back defect detection of substrates (b)–(c) in Fig.1 and/or 2. In the 8- μ m-thick nitride on Si (substrate (b)), the depth of the

cracks at the outermost periphery of the wafer is deep enough for Si substrates to be exposed at the bottom of the cracks. These deep cracks lead to large melt-back defects indicated by red arrows in this figure. On the contrary, the 8- μm -thick nitride on SiC/Si (substrate (c)) successfully attains no melt-back defects. As shown in Figs. 2 and 3, the 3C-SiC(111) intermediate layer was verified to exhibit excellent effects for suppressing cracks and melt-back defects, even in the case of a 8- μm -thick nitride and a practical 6" wafer.

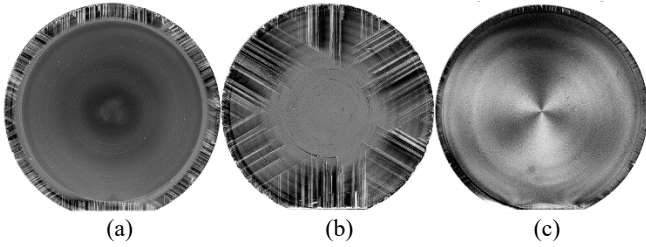


Fig.2 Laser scattering images by KLA-Tencor Candela CS20 for crack detection of (a) 7- μm -thick nitride on Si, (b) 8- μm -thick nitride on Si, and (c) 8- μm -thick nitride on SiC/Si.

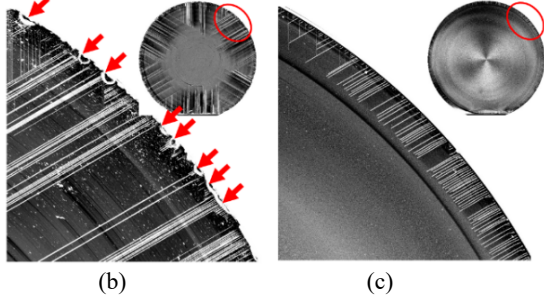


Fig.3 Extended laser scattering images by CS20 for melt-back defects detection (red arrows) of substrates (b)-(c) in Fig.1 or 2.

3. Electrical characteristics

The Hall measurement was conducted for the substrate (c), and excellent mobility (μ_c) of approximately 2000–2100 cm^2/Vs , sheet resistance (R_{sh}) of 500 $\Omega/\text{sq.}$ and a carrier concentration (N_s) of $6 \times 10^{12} / \text{cm}^2$ were obtained at room temperature.

The device structure, schematically shown in Fig. 4, was then fabricated on the 6" substrate (c). For the electrical measurements, devices with gate width, W_G , of 30 μm , and gate-drain length, L_{GD} , of 13 μm were used.

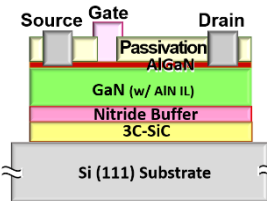


Fig.4 Schematic cross-section of AlGaN/GaN HEMT device structure fabricated on the substrate in Fig.1(c).

The wafer level off-leakage characteristics were measured, where the wafer temperature was maintained at 150 $^{\circ}\text{C}$, a negative gate bias was applied to turn off the device, source and back electrodes were grounded, and biases up to 600 V with 50-V steps were applied to the drain electrodes. Approximately 30 devices were measured on the wafer. Figure 5 shows the dependence on drain voltage, V_{DS} , of drain leakage current, I_D , which represents the sum of gate leakage current, I_G , source leakage current, I_S , and substrate leakage

current, I_{Sub} . All I_D data for V_{DS} up to 600 V are less than 10^{-7} A/mm, proving the commercial level off-leakage characteristics.

The current collapse characteristics were also measured for the substrates (c). In addition to Fig. 5, approximately 30 devices were measured on the wafer. In this measurement, the wafer was maintained at room temperature. The durations of the on- and off-states of the devices were maintained at 10 μs and 990 μs , respectively. In the off-states, biases up to 600 V with 50-V steps were applied to the drain electrodes. Figure 6 shows the dependence of the normalized dynamic R_{ON} on V_{DS} . The normalized dynamic R_{ON} successfully maintained practical values of less than 1.3 for all V_{DS} .

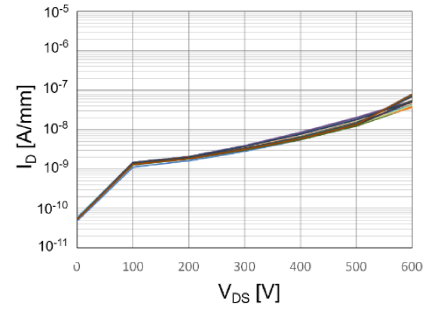


Fig.5 Dependence of I_D on V_{DS} at 150 $^{\circ}\text{C}$.

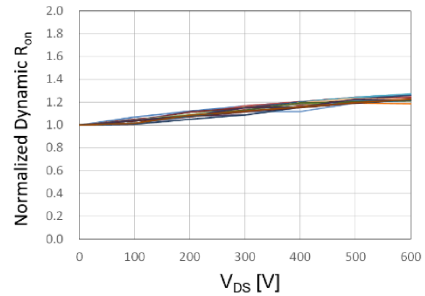


Fig.6 Current collapse characteristics at room temperature; dependence of normalized dynamic R_{ON} on V_{DS} .

4. Conclusions

Herein, we have grown 8- μm -thick nitride composite layers with a simple nitride buffer structure on the 6" 3C-SiC/Si substrates. The 3C-SiC intermediate layer exhibited excellent effects for suppressing cracks and melt-back defects, even in the case of the 8- μm -thick nitride and a practical wafer diameter of 6". The power HEMTs were fabricated on the wafers and practical off-leakage characteristics and current collapses were successfully confirmed. In addition, this thick-film GaN on SiC/Si exhibits excellent performance also in high-frequency applications, and the results will be reported in another abstract in this conference.

References

- [1] T. Takeuchi, H. Amano, K. Hiramatsu, N. Sawaki, and I. Akasaki, *J. Cryst. Growth* **115** (1991) 634.
- [2] J. Komiyama, Y. Abe, S. Suzuki, and H. Nakanishi, *Appl. Phys. Lett.* **88** (2006) 091901.
- [3] Y. Nakano *et al.*, *Abstracts of the 66th JSAP Spring Meeting* (2019) 11p-PB3-22, in Japanese.
- [4] K. Kawamura *et al.*, *Abstracts of IUMRS-ICEM 2016* (2016).